Application of the generalized semimicroscopic model to $1f_{7/2}$ nuclei

S. M. Abecasis* and Carlos A. Heras†
Laboratorio de Radiaciones, IIAE, Departamento de Física, Facultad de Ciencias Exactas y Naturales, Ciudad Universitaria, Pabellón I, Buenos Aires, Argentina

F. Krmpotić
Departamento de Física, Facultad de Ciencias Exactas, Universidad Nacional de La Plata, La Plata, Argentina
(Received 3 July 1974)

A detailed description with the generalized semimicroscopic model of the properties of the low-lying states of ^{49}Ti, ^{51}Cr, and ^{57}Co is performed. The last one is taken as a typical and well-known representative of the odd-mass cobalt isotopes. Calculated energy-level sequence, electromagnetic properties, spectroscopic factors, and lifetimes compare favorably with experiment.

[NUCLEAR STRUCTURE ^{49}T, ^{51}Cr, and ^{57}Co; calculated levels, J, π, S, q, μ, $B(E2)$, $B(M1)$, δ, b, and τ. Generalized semimicroscopic model.]

I. INTRODUCTION

The success obtained with the generalized semimicroscopic model (GSMM) when applied to odd-mass indium isotopes[1] (hereafter referred to as I) has encouraged us to explore the possibilities of its application to some $1f_{7/2}$ nuclei which are expected to be adequately described within this framework.

In the present investigation both a detailed description and a comparison of the properties of the low-lying states—energy-level sequence, electromagnetic properties, spectroscopic factors, and lifetimes—with experiment is performed for ^{49}Ti, ^{51}Cr, and ^{57}Co nuclei. The last one is taken as a typical and well-known representative of the odd-mass cobalt isotopes.

In the classical semimicroscopic model (SMM) these nuclei can be analyzed in terms of the coupling of a valence hole in the $N=28$ or $Z=28$ shell[2] coupled to the corresponding vibrational cores. In our version, some low-lying states which cannot be explained by the SMM are described by the coupling of a valence particle—which has available the orbits above the $1f_{7/2}$ shell—to the quadrupole vibrational field originated by a two-hole cluster in this shell coupled to collective harmonic surface oscillations.

To our knowledge, complete calculations for ^{49}Ti and ^{51}Cr have not been reported as yet. The shell-model calculations within the $1f_{7/2}$ shell made by McCullen, Bayman, and Zamick (MBZ)[3] reproduced the observed levels fairly well. However, the lowest $\frac{1}{2}-$ and $\frac{3}{2}-$ states are predicted too high in energy as compared with experiment. This would indicate that the mixing of the nearby $2p_{3/2}$, $2p_{1/2}$, and $1f_{5/2}$ orbits is of importance. The configuration mixing required can be figured out by the strong-coupling asymmetric-rotor model including the Coriolis coupling between bands as has been used by Malik and Scholz (MS).[4] The computed energy spectra for ^{49}Ti and ^{51}Cr compare favorably with experiment. In particular, the positions of the low-lying $\frac{1}{2}-$ and $\frac{3}{2}-$ states are predicted in the correct energy region. However, both approaches do not include calculations of electromagnetic properties and hence a more complete comparison with experiment cannot be made.

Concerning the odd-mass cobalt isotopes the situation—from the theoretical point of view—is quite different. In fact, a considerable amount of theoretical work has been devoted to them with different models ranging from pure shell-model calculations[5,6] to semimicroscopic approaches.[2,7-9] Although the calculations are complete and the agreement with the known properties of $^{57-63}$Co is good,[8,9] it appears pertinent for completeness to compare the results of our model with those obtained with other versions of the particle-phonon coupling model.

In Sec. II the formalism is summarized; the results obtained from the calculations for the nucleides ^{49}Ti, ^{51}Cr, and ^{57}Co are presented and discussed in Sec. III and finally, general conclusions are given in Sec. IV.

II. FORMALISM

Since detailed derivations of the formulas have been given in I, we only list here those expressions needed for the present applications.

The total Hamiltonian is

$$H = H(\text{core},h) + H(p) + H(p,h), \tag{1}$$

where $H(core,h)$ is associated with the system formed by one or two valence holes in the $1f_{7/2}$ shell coupled to collective quadrupole harmonic surface oscillations of the corresponding doubly even $A+1$ cores (^{50}Ti, ^{52}Cr, ^{58}Ni). For the one-hole case, it describes in the SMM the properties of ^{49}Ti, ^{51}Cr, and ^{57}Co isotopes. For the two-hole case, it describes in the SMM the properties of the doubly even $A-1$ nuclei (^{48}Ti, ^{50}Cr, ^{56}Fe). Let us remember that the GSMM is mainly based on the assumption that the two holes coupled to the quadrupole harmonic surface oscillations originate an average vibrational field which in turn is coupled to a valence particle which for the present case, has available the orbits $1f_{5/2}$, $2p_{3/2}$, and $2p_{1/2}$ lying above the $N=28$ ($Z=28$) major shell.

The Hamiltonian $H(p)$ represents the total energy of the valence particle, while the Hamiltonian $H(p,h)$ gives the coupling of the hole states to the two-hole–one-particle states.

Our base vectors are:

$$|h^{-1}, NR; IM\rangle = (|h^{-1}m_h\rangle \boxtimes |NRM_R\rangle)_{IM}, \tag{2}$$

$$|p, \tilde{N}\tilde{R}; IM\rangle = (|pm_p\rangle \boxtimes |\tilde{N}\tilde{R}M_{\tilde{R}}\rangle)_{IM}. \tag{3}$$

Here the symbols label:
(i) $|h^{-1}m_h\rangle$ and $|pm_p\rangle$, the state vectors of the fermions with h and p being the set of quantum numbers necessary to completely describe the valence-hole and valence-particle states with respect to the $N=28$ ($Z=28$) major shell;
(ii) $|NRM_R\rangle$ and $|\tilde{N}\tilde{R}M_{\tilde{R}}\rangle$, the state vectors of the $(A+1)$ and $(A-1)$ cores, respectively, assumed to be harmonic quadrupole vibrators;
(iii) $N \leq 3$ and $\tilde{N} \leq 2$, number of phonons;
(iv) R and $\tilde{R}$, quantum numbers of the resultant angular moments of N and $\tilde{N}$ phonons, respectively; and
(v) I and M, the total angular momentum quantum numbers of the ^{49}Ti, ^{51}Cr, and ^{57}Co isotopes.

The eigenstates of the total Hamiltonian can be written as

$$|^{\tau}IM\rangle = \sum_{hNR} \eta(h^{-1}, NR; {}^{\tau}I)|h^{-1}, NR; IM\rangle + \sum_{pN\tilde{R}} \eta(p, \tilde{N}\tilde{R}{}^{\tau}I)|p, \tilde{N}\tilde{R}; IM\rangle, \tag{4}$$

where τ distinguishes states of the same angular momentum I. The expansion coefficients η are obtained through diagonalization of the energy matrices given in I. With these eigenstates, the spectroscopic factors $(2I+1)S({}^{\tau}I)$ can be calculated as explained in I.

The reduced matrix elements of the electric quadrupole and magnetic dipole operators are expressed in the form

$$\langle I_f \| E2 \| I_i \rangle = A e^{\text{eff}} + B_1 e_{v1}^{\text{eff}} + B_2 e_{v2}^{\text{eff}}, \tag{5}$$

$$\langle I_f \| M_1 \| I_i \rangle = C g_R + D g_l + E g_s^{\text{eff}}, \tag{6}$$

where the indexes 1 and 2 stand for the $(A+1)$ and $(A-1)$ cores, respectively; e^{eff} is the effective nucleon charge expressed as a number times the proton charge e, and

$$e_{vi}^{\text{eff}} = (4\pi\beta/\sqrt{5}\, R_0^2)\, q_e = Ze\beta/\sqrt{5} \tag{7}$$

are the effective vibrator charges; Z is the number of protons, R_0 the radius, β the quadrupole deformation, and q_e the electric quadrupole moment, of the vibrating cores. The symbols g_R, g_l, and g_s^{eff} are the gyromagnetic ratios of the core, orbital, and spin parts, respectively. The quantities A, B_i, C, D, and E are calculated by means of the state vectors (4) and their explicit forms are given in I.

The mixing ratio δ^2 is calculated with the usual formula[10]

$$\delta^2 = 6.93\times10^{-5}\, E_\gamma^{\,2}\, \frac{B(E2)}{B(M1)}, \tag{8}$$

where the transition energy E_γ is given in MeV, $B(E2)$ in units of e^2 fm^4, and $B(M1)$ in $\mu_N{}^2$. The sign of δ is determined by the relative phase of the matrix elements (5) and (6).

The mean lifetimes of a state i is given by

$$\tau_i = 1/T_i, \tag{9}$$

where T_i is the total transition probability per unit time from the state. On the assumption that the internal conversion coefficients are negligible—which is valid except for very low transition energies—T_i can be expressed as

$$T_i = \sum_f T_{if}, \tag{10}$$

where the electromagnetic transition probability T_{if} to a particular state f is

$$T_{if} = \frac{4\pi}{75}\frac{1}{\hbar}\left(\frac{1}{\hbar c}\right)^5 B(E2; i\to f) E_\gamma{}^5 (1+1/\delta^2)\ (\text{fs}^{-1}), \tag{11}$$

where $\hbar$ is given in MeV fs, $\hbar c$ in MeV fm, E_γ in MeV, and $B(E2)$ in e^2 fm^4 with $e^2 = 1.4399$ MeV fm. Then, the numerical factor is 1.2254×10^{-6} MeV^{-6} fm^{-5} fs^{-1}. On the same assumption the branching ratio b_{if} of the decaying state i to the state f can

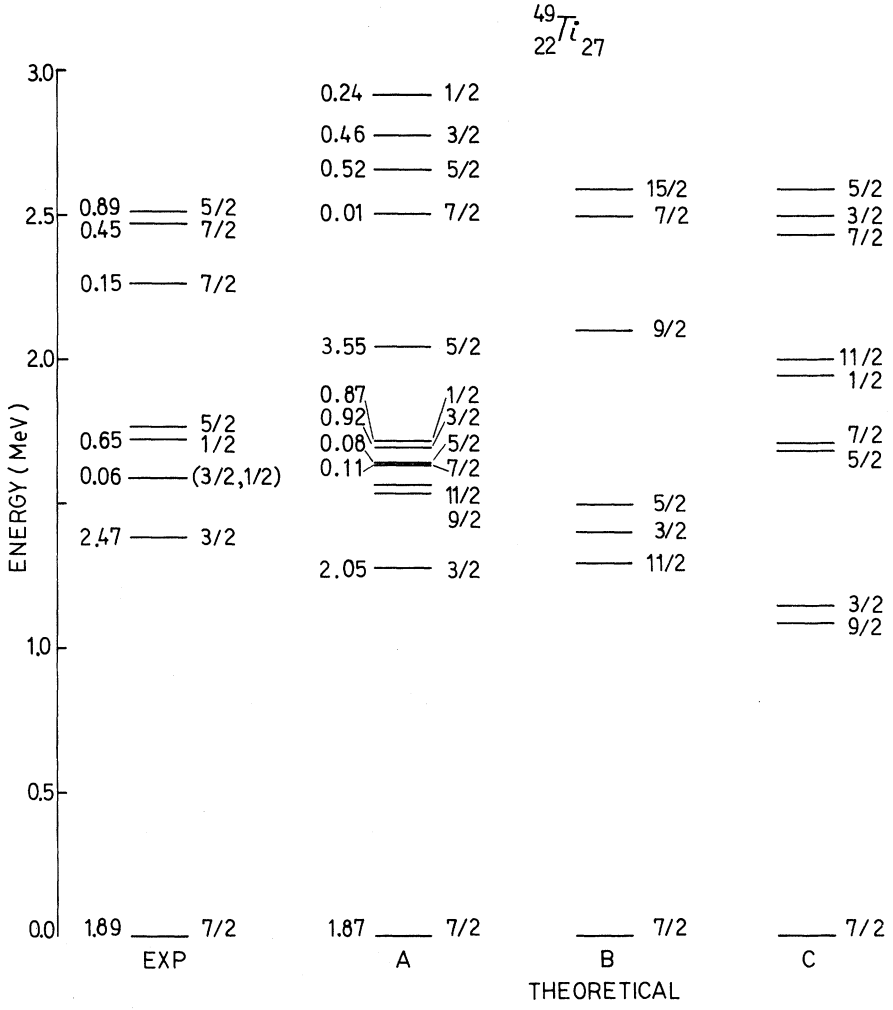

FIG. 1. Experimental (Ref. 14) and calculated low-lying negative-parity states in ^{49}Ti. The spectroscopic factors $(2I+1)$ S for the ^{48}Ti$(d,p)^{49}$Ti reaction (Ref. 14) are indicated at the left of each level. A: Present results for $\rho = 0.325$; $\epsilon(f_{7/2}) - \epsilon(p_{3/2}) = -1.767$ MeV; $\beta(^{50}\text{Ti}) = 0.175$; $\beta(^{48}\text{Ti}) = 0.290$; $\hbar\omega(^{50}\text{Ti}) = 1.58$ MeV; $\hbar\omega(^{48}\text{Ti}) = 0.983$ MeV; the other single-particle energies are indicated in the text. B: MBZ (Ref. 3) calculations. C: MS (Ref. 4) calculations for $\beta = 0.15$.

be conveniently written as

$$b_{if} = \tau_i T_{if} \ . \tag{12}$$

III. CALCULATIONS AND RESULTS

In our calculations, the energy difference $\Delta E = \epsilon(p_{3/2}) - \epsilon(f_{7/2})$ between the lowest unperturbed particle-like and hole-like states were estimated from the neutron (proton) separation energies of the particular nuclei, obtained from the tables Wapstra and Gove,[11] as explained in I.

The single-particle energies for both neutrons and protons were taken from the experimental level energies of ^{57}Ni (Ref. 12), namely, $\epsilon(f_{5/2}) - \epsilon(p_{3/2}) = 0.75$ MeV and $\epsilon(p_{1/2}) - \epsilon(p_{3/2}) = 1.05$ MeV. Therefore, we are neglecting the different ordering of neutron and proton orbits, the A dependence in the level positions, and the "fine structure" superimposed on it such as that yielded by the shift of the $f_{5/2}$ level relative to the $p_{3/2}$ and $p_{1/2}$ levels as one goes from $A = 49$ to $A = 57$ (Ref. 10).

The parameters β and the phonon energies $\hbar\omega$ were taken, respectively, as the quadrupole deformation and the energy of the $^12+$ states of the corresponding vibrators.[13]

Finally, rather than considering the radial integrals $\langle k_{\text{WS}} \rangle$, as generated from a Wood-Saxon potential with spin-orbit coupling, we modified

TABLE I. Components of the negative-parity states in ^{49}Ti below 3 MeV, shown in Fig. 1(A). Only components larger than 4% are listed.

τ_I	Energy (MeV)	$\lvert j, NR\rangle$ $\lvert \frac{7}{2}, 0\,0\rangle$	$\lvert \frac{5}{2}, 0\,0\rangle$	$\lvert \frac{3}{2}, 0\,0\rangle$	$\lvert \frac{1}{2}, 0\,0\rangle$	$\lvert \frac{7}{2}, 1\,2\rangle$	$\lvert \frac{5}{2}, 1\,2\rangle$	$\lvert \frac{3}{2}, 1\,2\rangle$	$\lvert \frac{1}{2}, 1\,2\rangle$	$\lvert \frac{7}{2}, 2\,2\rangle$	$\lvert \frac{7}{2}, 2\,4\rangle$
$1_{\frac{7}{2}}$	0.0000	−0.968				−0.239					
$1_{\frac{3}{2}}$	1.275			−0.716		−0.584		0.277			
$1_{\frac{9}{2}}$	1.536					−0.955					−0.240
$1_{\frac{11}{2}}$	1.564					−0.965					−0.223
$2_{\frac{7}{2}}$	1.633	−0.236				0.924					
$1_{\frac{5}{2}}$	1.640					0.980					
$2_{\frac{3}{2}}$	1.694			0.479		−0.754		−0.310		−0.244	
$1_{\frac{1}{2}}$	1.718				0.659		0.375	0.612			
$2_{\frac{5}{2}}$	2.045		−0.769				0.354	0.387	−0.289		
$3_{\frac{7}{2}}$	2.505							0.906		0.253	
$3_{\frac{5}{2}}$	2.661		0.293				−0.225	0.805		0.282	0.238
$3_{\frac{3}{2}}$	2.773			−0.338				−0.744			−0.482
$2_{\frac{1}{2}}$	2.922				−0.346		−0.457	0.500			0.626

their values by means of a parameter ρ in such a way as to obtain an over-all agreement of the predicted properties with experiment; so the following "effective" radial integrals $\langle k^{\text{eff}}\rangle$ were used

$$\langle k^{\text{eff}}\rangle = \rho\langle k_{\text{WS}}\rangle .$$

Throughout the calculations we used the following sets of effective values for the single-particle charges and gyromagnetic ratios, which are commonly used in the calculations in this region (the numbers between brackets refer to neutrons, the others to protons):

Set I $e^{\text{eff}} = e[0]$;
Set II $e^{\text{eff}} = 2e[0.5e]$;
Set 1 $g_R = 0\ [0]$, $g_s^{\text{eff}} = g_s^{\text{free}} = 5.59\ [-3.82]$;
Set 2 $g_R = 0\ [0]$, $g_s^{\text{eff}} = 0.6\, g_s^{\text{free}}\ [0.5\, g_s^{\text{free}}]$;
Set 3 $g_R = Z/A\ [Z/A]$, $g_s^{\text{eff}} = g_s^{\text{free}} = 5.59\ [-3.82]$;
Set 4 $g_R = Z/A\ [Z/A]$, $g_s^{\text{eff}} = 0.6\, g_s^{\text{free}}\ [0.5 g_s^{\text{free}}]$.

A. ^{49}Ti nucleus

In Fig. 1 the experimental negative-parity level sequence of ^{49}Ti is compared with the results of our calculation and with those obtained by MS and MBZ. The spectroscopic factors deduced for the ^{48}Ti$(d, p)^{49}$Ti reaction[14] are also compared. The main components of the low-lying negative-parity states are listed in Table I. Table II shows the calculated electric quardupole and magnetic dipole moments for the different sets of parameters.

As it is shown in Table I, the ground state and the first excited state are built mainly on the $\lvert f_{7/2}, 0\,0\rangle$ and $\lvert p_{3/2}, 0\,0\rangle$ configurations, respectively, while the $^1\frac{9}{2}$, $^1\frac{11}{2}$, $^2\frac{7}{2}$, $^1\frac{5}{2}$, and $^2\frac{3}{2}$ states are the members of the one-phonon multiplet $\lvert f_{7/2}, 1\,2; {}^nI\rangle$. The $^1\frac{1}{2}$ state has a particle-like nature, its main components being the $\lvert p_{1/2}, 0\,0\rangle$ and $\lvert p_{3/2}, 1\,2\rangle$ configurations.

Inspection of Fig. 1 shows that our calculations can account for the strong $l=1$ transitions in the (d, p) reaction to the low-lying $^1\frac{3}{2}$ and $^1\frac{1}{2}$ states at the observed energies 1.38 and 1.72 MeV, respectively. The level energies are in acceptable agreement with experiment but several additional levels are predicted. The theoretical $^2\frac{5}{2}$ state is expected to be strongly excited since it is based mainly on the $\lvert f_{5/2}, 0\,0\rangle$ configuration. However, the experimental results indicate a considerable fragmentation of the full $1f_{5/2}$ single-particle

TABLE II. Calculated static electric quadrupole and magnetic dipole moments in ^{49}Ti for some low-lying states shown in Fig. 1(A). The values of the effective charge and gyromagnetic ratios are indicated in the text. The available experimental data for the ground-state electric quadrupole and dipole magnetic moments are respectively, $Q = 0.24\,e$ b (Ref. 16) and $\mu = (-1.1036 \pm 0.0002)\mu_N$ (Ref. 18).

	Q (eb)		μ (μ_N)			
τ_I	I	II	1	2	3	4
$1_{\frac{1}{2}}$			0.6366	0.3183	0.7819	0.4636
$1_{\frac{3}{2}}$	−0.044 86	−0.054 16	−1.641	−0.8207	−1.757	−0.9366
$1_{\frac{5}{2}}$	0.027 05	0.046 08	−1.423	−0.7117	−1.466	−0.7540
$1_{\frac{7}{2}}$	0.083 26	0.1394	−1.892	−0.9458	−1.870	−0.9240
$2_{\frac{7}{2}}$	0.040 91	0.068 89	−1.525	−0.7627	−1.219	−0.4500
$1_{\frac{9}{2}}$	0.055 50	0.092 79	−1.674	−0.8372	−1.027	−0.1895
$1_{\frac{11}{2}}$	0.082 18	0.1377	−1.883	−0.9414	−0.9565	−0.0150

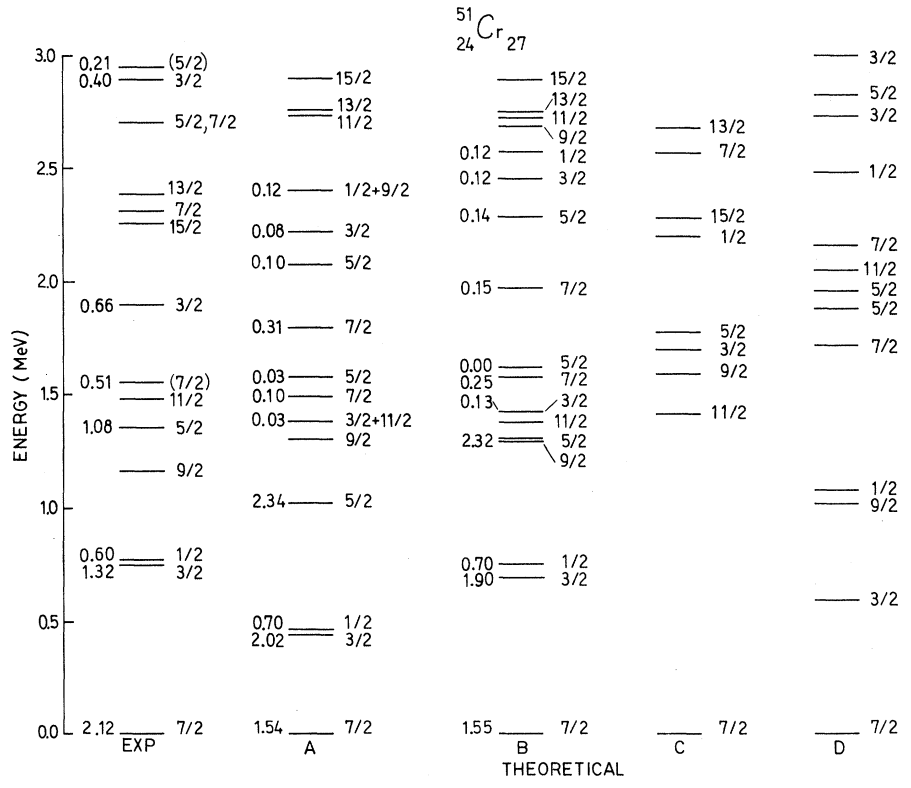

FIG. 2. Experimental (Refs. 19 and 20) and calculated low-lying negative-parity states in ^{51}Cr. The spectroscopic factors $(2I+1)$ S for the ^{50}Cr$(d,p)^{51}$Cr reaction (Ref. 12) are indicated at the left of each level. A and B: Present results. In A the energy $\epsilon(f_{7/2})$-$\epsilon(p_{3/2}) = -1.329$ MeV was obtained from the neutron separation energy whereas in B it was shifted down 300 keV. The values of the other parameters are: $\rho = 0.475$; $\beta(^{52}\text{Cr}) = 0.230$; $\beta(^{50}\text{Cr}) = 0.330$; $\hbar\omega(^{52}\text{Cr}) = 1.434$ MeV; $\hbar\omega(^{50}\text{Cr}) = 0.7831$ MeV; the other single-particle energies are indicated in the text. C: MBZ (Ref. 3) calculations. D: MS (Ref. 4) calculations for $\beta = 0.20$.

TABLE III. Components of the negative-parity states in ^{51}Cr below 3 MeV, shown in Fig. 2(b). Only components larger than 4% are listed.

τ_I	Energy (MeV)	$\lvert j, NR\rangle$ $\lvert \frac{7}{2}, 00\rangle$	$\lvert \frac{5}{2}, 00\rangle$	$\lvert \frac{3}{2}, 00\rangle$	$\lvert \frac{1}{2}, 00\rangle$	$\lvert \frac{7}{2}, 12\rangle$	$\lvert \frac{5}{2}, 12\rangle$	$\lvert \frac{3}{2}, 12\rangle$	$\lvert \frac{1}{2}, 12\rangle$	$\lvert \frac{7}{2}, 20\rangle$	$\lvert \frac{7}{2}, 22\rangle$	$\lvert \frac{3}{2}, 22\rangle$	$\lvert \frac{7}{2}, 24\rangle$	$\lvert \frac{5}{2}, 24\rangle$	$\lvert \frac{3}{2}, 24\rangle$	$\lvert \frac{1}{2}, 24\rangle$	$\lvert \frac{7}{2}, 33\rangle$	$\lvert \frac{7}{2}, 34\rangle$	$\lvert \frac{7}{2}, 36\rangle$
$1_{\frac{7}{2}}$	0.0000	0.881				0.432													
$1_{\frac{3}{2}}$	0.6959			0.690		−0.400		0.404	0.323										
$1_{\frac{1}{2}}$	0.7561				0.591		0.437	0.595											
$1_{\frac{9}{2}}$	1.299					0.856					−0.278		0.405						
$1_{\frac{5}{2}}$	1.313		−0.622				0.405	0.350	−0.434						−0.251				
$1_{\frac{11}{2}}$	1.381					0.876					0.207		0.396						
$2_{\frac{3}{2}}$	1.426			−0.180		0.741		0.356			0.434		0.220						
$2_{\frac{7}{2}}$	1.575	0.352				−0.690		0.343		−0.214	0.315								
$2_{\frac{5}{2}}$	1.622					0.862		0.292					0.321						
$3_{\frac{7}{2}}$	1.972	0.270				−0.205		−0.765		−0.266			−0.269		0.235	0.220			
$3_{\frac{5}{2}}$	2.287					0.412	0.233	−0.702	−0.256		−0.271	−0.209		−0.212					
$3_{\frac{3}{2}}$	2.451					−0.223		0.539	−0.531			0.211	0.426						
$2_{\frac{1}{2}}$	2.573				−0.243		−0.473	0.420					0.664					0.258	
$2_{\frac{9}{2}}$	2.688										0.807		0.419					0.281	0.216
$2_{\frac{11}{2}}$	2.726										−0.729		0.492				0.234	−0.350	0.214
$1_{\frac{13}{2}}$	2.751												−0.885						−0.409
$1_{\frac{15}{2}}$	2.893												0.905					0.220	0.364

TABLE IV. Calculated static electric quadrupole and magnetic dipole moments in ^{51}Cr for some low-lying states shown in Fig. 2(b). The values of the effective charge and gyromagnetic ratios are indicated in the text. The available experimental data is $\mu(\frac{1}{2}^-) = (-0.934 \pm 0.005)\mu_N$ [K. E. Adelroth and A. Rosen, Ark. Fyz. 40, 457 (1970)].

	Q (e b)		μ (μ_N)			
τ_I	I	II	1	2	3	4
$1_{\frac{1}{2}}$			0.6365	0.3182	0.7729	0.4547
$1_{\frac{3}{2}}$	−0.1226	−0.1388	−1.648	−0.8240	−1.521	−0.6972
$1_{\frac{5}{2}}$	−0.1831	−0.2188	1.093	0.5463	1.575	1.028
$1_{\frac{7}{2}}$	0.2309	0.2804	−1.839	−0.9195	−1.751	−0.8317
$2_{\frac{7}{2}}$	0.083 82	0.1043	−1.537	0.7682	−1.100	−0.3325
$1_{\frac{9}{2}}$	0.1399	0.1708	−1.592	−0.7960	−0.8310	−0.0350
$1_{\frac{11}{2}}$	0.2134	0.2610	−1.811	−0.9055	−0.7611	0.1444
$1_{\frac{13}{2}}$	0.083 53	0.1078	−1.491	−0.7456	0.2778	1.023

strength in the (d, p) reaction.[14] The theoretical results are not affected if the $f_{5/2}$-$f_{7/2}$ splitting is changed within reasonable limits (about ±400 keV). Due to the approximately 25% admixture of the $|p_{3/2}, 0\,0\rangle$ configuration in the state vector of the $^2\frac{3}{2}$ level we also predict that this state be the most strongly excited among the members of the first multiplet. On the other hand, the model can explain the strength of the $\frac{5}{2}$ state near 2.5 MeV, whereas the two $\frac{7}{2}$ levels experimentally found near this excitation energy cannot be satisfactorily accounted for.

The experimental electric quadrupole moment of the ground state equals +0.24 e b (Ref. 15) and compares favorably with the calculated value 0.14 e b for Set II (Table II), although no attempt to achieve the best fit was made. The observed ground-state magnetic dipole moment is $(-1.1036 \pm 0.002)\mu_N$ (Ref. 16), whereas the predicted value is $-0.94581\mu_N$ for Set. 2. Then the spin part is the only contribution and the sign comes from that of the spin gyromagnetic ratio.

Although a detailed agreement is not achieved it seems that the model is able to reproduce the general features of the low-lying spectrum in ^{49}Ti. In addition, the spectroscopic factors for all levels are given for the first time, and the appearance of the $^1\frac{3}{2}-$ and $^1\frac{1}{2}-$ states, not hitherto explained, is now correctly predicted.

Since additional experiment information on the decay properties of ^{49}Ti is not available, we omit the presentation of our calculations concerning them.[17] We only wish to point out that in spite of the inclusion of two-hole–one-particle excitations the predictions are qualitatively the same as those of the generalized vibrational intensity and selection rules (GVISR) of Alaga *et al.*[18] These rules are based on the lowest nonvanishing order of the rearranged perturbation series for the coupling of the vibrational field to shell-model clusters.

B. ^{51}Cr nucleus

The experimental and theoretical ^{51}Cr spectra and spectroscopic factors for the ^{50}Cr$(d, p)^{51}$Cr (Ref. 19) reaction are compared in Fig. 2. Part A displays our results obtained for $\epsilon(f_{7/2} - \epsilon(p_{3/2}) = -1.329$ MeV deduced from the neutron separation energies of ^{53}Cr and ^{51}Cr nuclei.[11] To obtain a better agreement with experiment a shift down of 300 keV in this value was allowed. The results obtained in this case are shown in part B. The corresponding state vectors for some of the low-lying negative-parity states are presented in Table III. The electromagnetic properties are given in Tables IV and V for two different sets of the parameters.

The ground state of ^{51}Cr is based on the $|f_{7/2}, 0\,0\rangle$ configuration, whereas the $^1\frac{3}{2}$ and $^1\frac{1}{2}$ states are mainly formed by $|p_{3/2}, 0\,0\rangle$, and $|p_{1/2}, 0\,0\rangle$, and $|p_{3/2}, 1\,2\rangle$ configurations, respectively. In this way we have a simple explanation of the occurrence of these levels at low excitation energy. The nature of the $^1\frac{5}{2}$ level also explains its strength in the (d, p) reaction in agreement with the experimental data. The other experimental excited states around

TABLE V. Decay properties of ^{51}Cr. For each transition between levels shown in Fig. 2(b), the first row gives the calculated values and the second, the available experimental results. The values of the effective charge and gyromagnetic ratios are indicated in the text. Weisskopf units (Ref. 11) are indicated W.u.

Transition τ_{I_i} τ'_{I_f}	$B(E2)$ (W.u.) I	II	$B(M1)$ (W.u.)[a] 2	3	δ[a] 1+3	1+2	b (%)[a] 1+3	1+2	τ (fs) 1+3	1+2
$1\frac{3}{2}$ $1\frac{7}{2}$	4.40	3.87					100	100	1.01×10^5	1.15×10^5
	0.0419 ± 0.002[b]								$(7.35\pm0.03)\times10^6$[c]	
$1\frac{1}{2}$ $1\frac{3}{2}$	15.5	20.5	0.162	0.734	−0.006	−0.014	100	100	3.77×10^5[d]	1.71×10^6[d]
									$(5.53\pm0.07)\times10^6$[c]	
$1\frac{9}{2}$ $1\frac{7}{2}$	14.9	16.5	0.004	0.057	0.392	1.59	100	100	176	856
	12^{+6}_{-3}[a]		$0.24^{+0.10}_{-0.06}$		$0.17^{+0.02}_{-0.01}$					82^{+30}_{-26}[e]
$1\frac{5}{2}$ $1\frac{1}{2}$	7.51	10.6					0.3	2		
$1\frac{5}{2}$ $1\frac{3}{2}$	3.02	3.90	0.001	0.006	−0.244	−0.587	3.4	4	519	2296
					-0.25 ± 0.05				550^{+250}_{-150}[f]	>850[e]
$1\frac{5}{2}$ $1\frac{7}{2}$	0.160	0.116	0.006	0.026	0.068	0.124	96.3	94		
$1\frac{11}{2}$ $1\frac{9}{2}$	2.05	3.12	0.014	0.188	0.005	0.024	0.4	0		
	<25[a]		$0.50^{+0.50}_{-0.13}$		-0.03 ± 0.03		50		1077	1071
$1\frac{11}{2}$ $1\frac{7}{2}$	13.4	13.5					99.6	100		800^{+510}_{-310}[e]
	6^{+4}_{-2}[a]						50			
$2\frac{3}{2}$ $1\frac{5}{2}$	0.596	1.06	0.000	0	∞	−0.459	0	0		
$2\frac{3}{2}$ $1\frac{1}{2}$	0.142	0.445	0.035	0.180	0.009	0.035	77	44	225	653
$2\frac{3}{2}$ $1\frac{3}{2}$	4.37	5.82	0.000	0.017	+0.248	−2.52	5	1	550^{+120}_{-90}[f]	370^{+174}_{-88}[e]
$2\frac{3}{2}$ $1\frac{7}{2}$	9.97	10.4					18	55		
$2\frac{7}{2}$ $2\frac{3}{2}$	0.743	0.890					0	0		
$2\frac{7}{2}$ $1\frac{11}{2}$	0.009	0.107					0	0		
$2\frac{7}{2}$ $1\frac{5}{2}$	0.434	0.427	0.001	0.008	0.035	0.118	0.25	0.00	407	793
$2\frac{7}{2}$ $1\frac{9}{2}$	3.79	5.22	0.025	0.321	−0.020	−0.083	9	1	>4000[f]	>412[e]
$2\frac{7}{2}$ $1\frac{3}{2}$	2.49	2.37					0.75	1		
$2\frac{7}{2}$ $1\frac{7}{2}$	8.92	8.38	0.001	0.008	−1.07	−3.21	90	97		
$1\frac{13}{2}$ $2\frac{9}{2}$	0.019	0.032					0	0		
$1\frac{13}{2}$ $1\frac{11}{2}$	9.24	10.6	0.005	0.079	0.287	1.18	84	42	104	351
					0.07 ± 0.02					95^{+30}_{-21}[f]
$1\frac{3}{2}$ $1\frac{9}{2}$	17.6	18.4					16	58		

TABLE V *(Continued)*

Transition τ_{I_i} τ'_{I_f}	$B(E2)$ (W.u.) I	II	$B(M1)$ (W.u.) [a] 2	3	δ [a] 1+3	1+2	b (%) [a] 1+3	1+2	τ (fs) 1+3	1+2
$1^{\frac{15}{2}}$ $1^{\frac{13}{2}}$	1.41	2.50	0.020	0.276	0.006	0.031	1	0	365	363
$1^{\frac{15}{2}}$ $1^{\frac{11}{2}}$	24.9	25.3					99	100	>1000 [f]	>100 [e]

[a] Reference 22.
[b] Calculated from experimental data assuming a negligible total conversion coefficient.
[c] W. Haar and F. W. Richter, Z. Phys. 231, 1 (1970).
[d] Calculated with a total conversion coefficient $\alpha = 0.906$ [M. E. Rose, *Internal Conversion Coefficients* (North-Holland, Amsterdam, 1958)].
[e] K. V. K. Iyengar and B. C. Robertson, Nucl. Phys. A174, 385 (1971).
[f] Reference 5.

1.5 MeV can be explained as members of the one-phonon multiplet $|f_{7/2}, 1\,2, {}^{n}I\rangle$. In general, the level sequence and spectroscopic factors obtained with the calculated state vectors follow closely the trend of experimental data.

The rather large negative quadrupole moments of the $1^{\frac{3}{2}}$, $1^{\frac{5}{2}}$, $3^{\frac{7}{2}}$, and $2^{\frac{9}{2}}$ states and the enhanced $E2$ transitions between some of them favor the assumption of a quasirotational structure in coexistence with the quasivibrational structure, a fact which is generally established by the GSMM.[1] The predicted value for the set ground-state dipole magnetic moment agrees with the experimental value for the 2 and is rather independent of g_R (Table V). As it was to be expected, this is consistent with the results for ^{49}Ti.

The calculated values of $B(E2)$ agree with the few measured ones.[20] Then, due to the scarcity of experimental information we discuss them qualitatively referring to the GVISR of Alaga *et al.*[18]

The transitions $1^{\frac{3}{2}} \rightarrow 1^{\frac{7}{2}}$, $1^{\frac{5}{2}} \rightarrow 1^{\frac{3}{2}}$, and $1^{\frac{5}{2}} \rightarrow 1^{\frac{7}{2}}$ are predominantly particle transitions with $\Delta N = 0$, $N = 0$. They are hindered by different amounts: In the first case the collective and particle contributions are out of phase, as the absolute value of the difference of the single-particle energies is greater than the phonon energy; in the second because of spin flip, and in the latter for both reasons.

The transitions $1^{\frac{9}{2}} \rightarrow 1^{\frac{7}{2}}$, $1^{\frac{11}{2}} \rightarrow 1^{\frac{7}{2}}$, $2^{\frac{3}{2}} \rightarrow 1^{\frac{7}{2}}$, $2^{\frac{7}{2}} \rightarrow 1^{\frac{7}{2}}$, and $2^{\frac{5}{2}} \rightarrow 1^{\frac{7}{2}}$, all with $\Delta N = 1$, $N = 1 \rightarrow N = 0$; and $1^{\frac{13}{2}} \rightarrow 1^{\frac{11}{2}}$, $1^{\frac{13}{2}} \rightarrow 1^{\frac{9}{2}}$, and $1^{\frac{15}{2}} \rightarrow 1^{\frac{11}{2}}$ with $\Delta N = 1$, $N = 2 \rightarrow N = 1$, are predominantly collective $E2$ transitions and consequently are expected to be enhanced.

In Table V we only show the results of $B(M1)$ strengths corresponding to the Sets 2 and 3 of parameters because the first gives the correct value of the ground-state dipole magnetic moment, and together with the second practically covers the whole range of calculated $B(M1)$ values. For the same reason, the combinations indicated in the last three columns were chosen. The omitted combinations yield similar results. The only available experimental values of $B(M1)$ strengths and mixing ratios (see previous footnote) are not well reproduced with the Set 2. This lack of agreement is not conclusive. In this respect, further experimental work would be highly desirable. Concerning the branching ratios b, nothing can be stated since the only quoted value for the $1^{\frac{11}{2}-}$ state is an assumption to calculate[21] $B(E2)$ from the measured lifetime. The experimental lifetimes are in general reasonably well accounted for. The only manifest discrepancy is that of the $1^{\frac{3}{2}}$ state.

C. ^{57}Co nucleus

Since most of the experimental data for odd-mass cobalt isotopes refer to ^{57}Co we limit the following discussion to this nucleus.

The experimental level sequence and spectroscopic factors for the ^{56}Fe(^{3}He, d)^{57}Co (Ref. 22) are compared in Fig. 3(a) with the present calculated values. To facilitate comparison with the predictions of other versions of the particle-phonon coupling model, the results obtained by Satpathy and Gujrathi,[2] Stewart, Castel, and Singh,[8] and Gómez[9] are also presented in parts B, C, and D, respectively. In Table VI the state vectors of the low-lying negative-parity states in ^{57}Co are given. The electric quadrupole and magnetic dipole moments are shown in Table VII.

Table VIII displays the values of $B(E2)$, $B(M1)$, mixing and branching ratios, and lifetimes for the states below 3 MeV in ^{57}Co. For comparison, available experimental information is also given.

The pairs of levels $1^{\frac{9}{2}}$, $1^{\frac{3}{2}}$ and $1^{\frac{1}{2}}$, $1^{\frac{11}{2}}$ are predicted at the correct energy region but with in-

verted order in each pair. The same situation appears in Gómez's calculations, whereas in those of Stewart *et al.* the right correspondence is obtained. (It is to be noted that in ^{59}Co the first pair has the spin sequence $\frac{3}{2}$, $\frac{9}{2}$.)

The two low-lying $\frac{3}{2}$ states show a conflicting point between our predictions and the observed properties. The spectroscopic factors in the stripping reaction ^{56}Fe(^{3}He, d) (Ref. 22) and the $B(E2)$ values (Table VIII) indicate that the lower one is mainly of single-particle nature, whereas we predict the inverse situation. However, in the ^{58}Ni(t, α)^{57}Co reactions,[23] the $^2\frac{3}{2}$ state is the most strongly excited. It is interesting to point out that in the case of ^{59}Co the observed $^1\frac{3}{2}$ state appears to have a collective nature, which is described by the present model. The other single-particle strengths in the stripping reaction are reasonably well reproduced except for the $^3\frac{7}{2}$ state predicted at 2.64 MeV.

No experimental data on quadrupole moments are available for ^{57}Co, but the calculated values for the ground state (Table VII) compares favorably with that measured in ^{59}Co, $Q = 0.39 \pm 0.06$ eb (Ref. 24). It is expected that the ground state in both isotopes has a similar structure, and this is the situation predicted by our model.

The relatively large negative quadrupole moments of the states $^2\frac{3}{2}$, $^2\frac{5}{2}$, and $^3\frac{9}{2}$ (predicted at 4.00 MeV) and the fairly enhanced $E2$ transition probabilities between them and to the $^1\frac{1}{2}$ state would indicate a quasirotational structure as in ^{51}Cr (see above). The magnetic dipole moments of the ground and $^2\frac{3}{2}$ states are correctly reproduced for a given set of parameters (Table VII).

The calculated $B(E2)$ strengths agree with experiment in four cases out of the nine reported ones. As mentioned above, the main discrepancies concern the ground-state $E2$ transitions from the $^1\frac{3}{2}$ and $^2\frac{3}{2}$ states. On the other hand, the $^1\frac{3}{2}$ state belongs, together with the $^1\frac{5}{2}$, $^2\frac{7}{2}$, $^1\frac{9}{2}$, and $^1\frac{11}{2}$ states, to the one-phonon multiplet based on the ground-state configuration (Table VI). Therefore, according to the GVISR[18] the $E2$ transitions to the ground-state from the $^1\frac{3}{2}$, $^1\frac{9}{2}$, and $^1\frac{11}{2}$ states should be allowed whereas the remaining ones

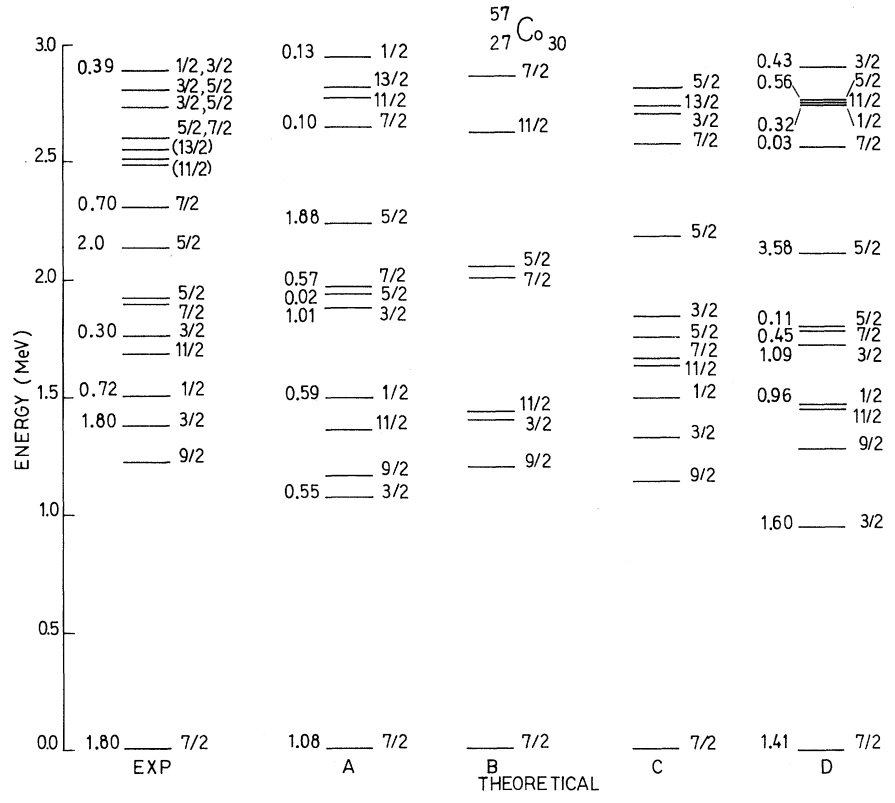

FIG. 3. Experimental (Ref. 21) and calculated low-lying negative-parity states in ^{57}Co. The spectroscopic factors $(2I+1)$ S for the ^{56}Co(^{3}He, d)^{57}Co reaction (Ref. 21) are indicated at the left of each level. A: Present results for $\rho = 0.875$; $\epsilon(f_{7/2}) - \epsilon(p_{3/2}) = -2.603$ MeV; $\beta(^{58}\text{Ni}) = 0.187$; $\beta(^{56}\text{Fe}) = 0.230$; $\hbar\omega(^{58}\text{Ni}) = 1.453$ MeV; $\hbar\omega(^{56}\text{Fe}) = 0.847$ MeV; the other single-particle energies are indicated in the text. B, C, and D: Results presented in Refs. 2, 8, and 9, respectively.

TABLE VI. Components of the negative-parity states in ^{57}Co below 3 MeV, shown in Fig. 3(a). Only components larger than 4% are listed.

τ_I	Energy (MeV)	$\lvert j, NR\rangle$ $\lvert\frac{7}{2}, 0\,0\rangle$	$\lvert\frac{5}{2}, 0\,0\rangle$	$\lvert\frac{3}{2}, 0\,0\rangle$	$\lvert\frac{1}{2}, 0\,0\rangle$	$\lvert\frac{7}{2}, 1\,2\rangle$	$\lvert\frac{5}{2}, 1\,2\rangle$	$\lvert\frac{3}{2}, 1\,2\rangle$	$\lvert\frac{1}{2}, 1\,2\rangle$	$\lvert\frac{7}{2}, 2\,0\rangle$	$\lvert\frac{7}{2}, 2\,2\rangle$	$\lvert\frac{7}{2}, 2\,4\rangle$	$\lvert\frac{3}{2}, 2\,4\rangle$	$\lvert\frac{7}{2}, 3\,2\rangle$	$\lvert\frac{7}{2}, 3\,3\rangle$	$\lvert\frac{7}{2}, 3\,6\rangle$
$1_{\frac{7}{2}}$	0.0000	0.735				0.588						0.202				
$1_{\frac{3}{2}}$	1.071			0.372		0.725					0.452					
$1_{\frac{9}{2}}$	1.165					0.735					0.346	−0.512				
$1_{\frac{11}{2}}$	1.359					−0.751					−0.253	−0.533				−0.213
$1_{\frac{1}{2}}$	1.494				0.541		0.424	0.575				0.326				
$2_{\frac{3}{2}}$	1.875			−0.503				0.513	0.300		0.327	0.353				
$1_{\frac{5}{2}}$	1.935					0.712		0.241			0.337	0.469			0.205	
$2_{\frac{7}{2}}$	1.967	0.535				−0.391		0.257		−0.311	0.434	−0.275		−0.259		
$2_{\frac{5}{2}}$	2.236		0.559				−0.401	−0.326	0.455							
$3_{\frac{7}{2}}$	2.643	0.226						−0.428		−0.364	−0.526	−0.388		−0.208	−0.252	
$2_{\frac{11}{2}}$	2.768					−0.592					0.326	0.437		0.211	−0.359	0.393
$1_{\frac{13}{2}}$	2.813											0.821			−0.230	0.500

should be hindered, and this is reflected in our calculations.

The available $B(M1)$ strengths are fairly well reproduced by our calculations. The Sets 2 and 3 have been chosen as a kind of compromise to describe the experimental data on dipole magnetic moments and transitions. For almost all transitions the correct sign and magnitude of the mixing ratio δ is predicted.

As for the branching ratios b a detailed agreement could not be achieved with any of the possible combinations of parameters. In fact, the values are rather independent of the set chosen. Lifetimes τ are predicted, in general, within the order of magnitude of the experimental value; there is accord in several cases and the only two manifest discrepancies occur for the $^1\frac{3}{2}$ and $^1\frac{1}{2}$ states. This situation does not depend on the set of parameters used because calculated lifetimes vary very slowly with the parameters, except in the case of the $^1\frac{1}{2}$ state for which the values shown cover the range of results.

IV. GENERAL CONCLUSIONS

As mentioned in the Introduction, no extensive calculations exist for ^{49}Ti and ^{51}Cr, whereas several are available with different models for the odd-mass cobalt isotopes. Semimicroscopic approaches based on harmonic vibrations of the $A+1$ cores failed to explain many features of the level spectra below about 2 MeV. The success of Stewart *et al.*[8] in describing odd-mass cobalt isotopes by including quasiparticles in upper orbitals together with anharmonic effects, suggests that excitations other than those considered by the classical SMM are needed in order to explain observed properties. In our model we consider that the additional excitations are the two-hole–one-particle ones, and represent them by the states of a particle interacting with the $A-1$ vibrating core, Eq. (3). When calculating cross matrix elements between these states and the hole-like states, Eq. (2), we approximate them by states of the $A+1$ vibrating core coupled to the $f_{7/2}$-shell two-hole states with zero angular momentum. This approximation appears to be justified since a general result in semimicroscopic calculations is that in the lowest states these configurations carry most of the strength.[25]

Low spin negative-parity levels at low energies are satisfactorily described, particularly the $^1\frac{1}{2}$ one which is practically built on two-hole–one-particle configurations in all three nuclei. The calculated lifetimes, however, are shorter than observed in ^{51}Cr and ^{57}Co (no data exist for ^{49}Ti). This same situation was found by Stewart *et al.*[8] for the $^1\frac{1}{2}$ state of cobalt isotopes. The second $\frac{3}{2}$ observed level is predicted collective in nature, whereas the first is mainly of particle nature. As pointed out above, in the case of ^{57}Co the prediction is the reverse of that indicated by experiment. It would then be highly desirable if measurements on the decay properties of the $^2\frac{3}{2}$ level in ^{49}Ti and ^{51}Cr were performed.

It is worth mentioning that for almost all transitions, the mixing ratios δ are predicted with the correct sign, and in many cases with the correct magnitude too. Concerning the branching ratios no general conclusions can be drawn, since only for ^{57}Co experimental data are available, and in this case a partial agreement is obtained.

Another feature of our calculations, already found for the odd-mass indium isotopes,[1] are (i) the appearance of a quasirotational structure—as suggested by the relatively large negative quadrupole moments of some states and the enhanced $E2$ transitions between them, and (ii) a consistency with the GVISR,[17] based on approximate expressions for the $E2$ transition probabilities.

A point worth emphasizing is that a fairly good agreement has been achieved with only one free

TABLE VII. Calculated electric quadrupole and magnetic dipole moments in ^{57}Co for some low-lying states shown in Fig. 3(a). The sets of effective values for the single-particle charge and gyromagnetic ratios are indicated in the text. The experimental values for the dipole magnetic moments of the ground state and the $^2\frac{3}{2}^-$ states are $(4.722\pm0.017)\mu_N$ [Z. Nielsen and W. J. Huiskamp, Physica 57, 1 (1972)] and $(3.0\pm0.06)\mu_N$ (Ref. 18), respectively.

	Q (e b)		μ (μ_N)			
τ_I	I	II	1	2	3	4
$^1\frac{1}{2}$			−0.674	−0.327	−0.472	−0.125
$^1\frac{3}{2}$	0.108	0.130	4.03	3.22	3.65	2.85
$^2\frac{3}{2}$	−0.098	−0.126	2.39	1.68	2.72	2.01
$^1\frac{5}{2}$	0.089	0.098	3.34	2.71	3.61	2.98
$^2\frac{5}{2}$	−0.257	−0.324	0.131	0.672	0.710	1.25
$^1\frac{7}{2}$	0.436	0.519	5.21	4.26	5.39	4.44
$^2\frac{7}{2}$	0.200	0.258	4.69	3.82	5.05	4.18
$^1\frac{9}{2}$	0.230	0.277	4.45	3.64	5.35	4.54
$^1\frac{11}{2}$	0.357	0.432	5.06	4.14	6.27	5.35
$^1\frac{13}{2}$	0.138	0.179	4.34	3.56	6.25	5.46

TABLE VIII. Decay properties of ^{57}Co. For each transition between the levels shown in Fig. 3(a), the first row gives the calculated values and the second, the available experimental results. The values of effective charge and gyromagnetic ratios are indicated in the text. Weisskopf units (Ref. 11) are indicated W.u.

Transition τ_{I_i} τ'_{I_f}	$B(E2)$ (W.u.) [a] I	II	$B(M1)$ (W.u.) [a] 2	3	δ [a,b] 1+2	1+3	b (%) [b] 1+2	1+3	τ (fs) [a] 1+2	1+3
$1_{\frac{3}{2}}$ $1_{\frac{7}{2}}$	13.1	13.2					100	100	3.39×10^3	3.39×10^3
	0.45 ± 0.08 [c]						100		$(28\pm5)\times10^3$ [d]	
$1_{\frac{9}{2}}$ $1_{\frac{7}{2}}$	21.4	26.2	0.237	0.172	−0.222	−0.262	100	100	64	87
	18	±4	0.19 ± 0.04		-0.27 ± 0.01		100		84 ± 18	
$1_{\frac{11}{2}}$ $1_{\frac{9}{2}}$	6.29	9.46	0.379	0.280	−0.016	−0.019	9	7		
	39	±2	0.5	±0.2	-0.09 ± 0.01		56 ± 3		884	906
$1_{\frac{11}{2}}$ $1_{\frac{7}{2}}$	13.9	14.16					91	93	260^{+120}_{-90}	
	10	±4					44 ± 3			
$1_{\frac{1}{2}}$ $1_{\frac{3}{2}}$	12.7	15.6	0.013	0.074	0.292	0.125	100	100	29	$\times10^3$ 5547
			0.02				100		$(866\pm72)\times10^3$ [d]	
$2_{\frac{3}{2}}$ $1_{\frac{1}{2}}$	6.07	10.2	0.358	0.668	−0.025	−0.018	51	75		
							<2			
$2_{\frac{3}{2}}$ $1_{\frac{3}{2}}$	13.5	17.5	0.026	0.0002	−0.415	−4.96	20	2	406	319
							0		360 ± 70	
$2_{\frac{3}{2}}$ $1_{\frac{7}{2}}$	1.94	2.35					29	23		
	10	±2					>98			
$1_{\frac{5}{2}}$ $2_{\frac{3}{2}}$	0.32	0.91	0.259	0.176	−0.001	−0.001	0	0		
$1_{\frac{5}{2}}$ $1_{\frac{1}{2}}$	0.41	0.45					0	0		
$1_{\frac{5}{2}}$ $1_{\frac{9}{2}}$	5.32	6.69					0	0		
							0		13	16
									30 ± 20	
$1_{\frac{5}{2}}$ $1_{\frac{3}{2}}$	12.4	16.4	0.414	0.326	−0.087	−0.098	16	16		
							0			
$1_{\frac{5}{2}}$ $1_{\frac{7}{2}}$	3.15	1.75	0.278	0.218	−0.146	−0.165	84	84		
							100			
$2_{\frac{7}{2}}$ $1_{\frac{5}{2}}$	1.46	2.07	0.049	0.034	−0.003	−0.004	0	0		
							0			
$2_{\frac{7}{2}}$ $2_{\frac{3}{2}}$	1.83	1.86					0	0		

TABLE VIII *(Continued)*

Transition τ_{I_i} τ'_{I_f}	$B(E2)$ (W.u.) [a] I	II	$B(M1)$ (W.u.) [a] 2	3	δ [a,b] 1+2	1+3	b (%) [b] 1+2	1+3	τ (fs) [a] 1+2	1+3
$2^{7}_{\frac{2}{2}}$ $1^{11}_{\frac{2}{2}}$	0.02	0.17					0	0		
									64	76
$2^{7}_{\frac{2}{2}}$ $1^{9}_{\frac{2}{2}}$	7.35	10.3	0.404	0.311	0.077	0.088	42	39	120 ± 30	
	1	± 1	0.6	± 0.2	-0.02 ± 0.01		60 ± 7			
$2^{7}_{\frac{2}{2}}$ $1^{3}_{\frac{2}{2}}$	0.72	0.59					0	0		
$2^{7}_{\frac{2}{2}}$ $1^{7}_{\frac{2}{2}}$	4.34	3.28	0.029	0.025	0.542	0.587	57	61		
			0.02	± 0.01			40 ± 7			
$2^{5}_{\frac{2}{2}}$ $2^{7}_{\frac{2}{2}}$	0.91	0.96	0.008	0.004	0.067	0.090	0.14	0.05		
$2^{5}_{\frac{2}{2}}$ $1^{5}_{\frac{2}{2}}$	0.01	0.05	0.011	0.010	-0.006	-0.006	0.30	0.17		
$2^{5}_{\frac{2}{2}}$ $2^{3}_{\frac{2}{2}}$	3.08	5.01	0.012	0.019	0.106	0.084	0.84	0.84		
$2^{5}_{\frac{2}{2}}$ $1^{1}_{\frac{2}{2}}$	12.9	19.9					1.44	0.90		
									311	194
							3	± 1		
$2^{5}_{\frac{2}{2}}$ $1^{9}_{\frac{2}{2}}$	0.17	0.11					0.12	0.07		
							0			
$2^{5}_{\frac{2}{2}}$ $1^{3}_{\frac{2}{2}}$	1.17	2.02	0.0001	0.001	2.40	0.727	2	3		
					$0.34^{+0.20}_{-0.11}$		14 ± 5			
$2^{5}_{\frac{2}{2}}$ $1^{7}_{\frac{2}{2}}$	0.01	0.00	0.009	0.014	-0.047	-0.037	95	95		
					0.06 ± 0.07		83 ± 4			
$3^{7}_{\frac{2}{2}}$ $2^{5}_{\frac{2}{2}}$	0.10	0.24	0.120	0.201	-0.007	-0.006	2	4		
$3^{7}_{\frac{2}{2}}$ $2^{7}_{\frac{2}{2}}$	1.00	1.56	0.004	0.0003	-0.230	-0.818	0.20	0.04		
$3^{7}_{\frac{2}{2}}$ $1^{5}_{\frac{2}{2}}$	0.92	1.37	0.300	0.220	-0.024	-0.028	21	22		
$3^{7}_{\frac{2}{2}}$ $2^{3}_{\frac{2}{2}}$	0.05	0.14					0	0		
							0			
$3^{7}_{\frac{2}{2}}$ $1^{11}_{\frac{2}{2}}$	6.68	6.81					2	2	46	66
							0		320 ± 90	
$3^{7}_{\frac{2}{2}}$ $1^{9}_{\frac{2}{2}}$	1.29	1.04	0.026	0.020	-0.237	-0.266	13	15		
	$1.5^{+1.3}_{-0.7}$ [c]		0.05	± 0.02	-0.13 ± 0.02		68 ± 2			
$3^{7}_{\frac{2}{2}}$ $1^{3}_{\frac{2}{2}}$	12.6	14.8					9	13		
	23^{+13}_{-7} [c]						8 ± 1			
$3^{7}_{\frac{2}{2}}$ $1^{7}_{\frac{2}{2}}$	0.03	0.02	0.020	0.011	0.074	0.098	53	44		

TABLE VIII *(Continued)*

Transition τ_{I_i} τ'_{I_f}	$B(E2)$ (W.u.) [a] I	II	$B(M1)$ (W.u.) [a] 2	3	δ [a,b] 1+2	1+3	b (%) [b] 1+2	1+3	τ (fs) [a] 1+2	1+3
	$0.10^{+0.47}_{-0.08}$ [c]				0.4 ±0.6		24 ±3			
$2_{11/2}$ $3_{7/2}$	0	0					0	0		
$2_{11/2}$ $2_{7/2}$	0.40	0.65					0	0		
$2_{11/2}$ $1_{11/2}$	7.02	8.92	0.038	0.028	−0.429	−0.502	10	10	24	33
$2_{11/2}$ $1_{9/2}$	22.7	26.5	0.211	0.151	−0.341	−0.403	90	90		
$2_{11/2}$ $1_{7/2}$	0	0					0	0		
$1_{13/2}$ $2_{11/2}$	0.76	1.51	0.223	0.166	−0.002	−0.002	9	12		
$1_{13/2}$ $1_{11/2}$	12.5	16.4	0.305	0.219	−0.194	−0.229	91	88	25	34
$1_{13/2}$ $1_{9/2}$	17.8	20.0					0	0		

[a] K. S. Burton and L. C. McIntyre, Jr., Phys. Rev. C 3, 621 (1971), unless otherwise stated.
[b] K. L. Coop, I. G. Graham, and E. W. Titterton, Nucl. Phys. A149, 463 (1970).
[c] Calculated from experimental data assuming a negligible total conversion coefficient.
[d] Reference 13.

parameter, ρ, introduced phenomenologically in order to improve the agreement with experiment. Obviously, a better agreement would be obtained by changing all the parameters of the model (single-particle and phonon energies, etc.) but this was considered unnecessary due to the exploratory nature of the calculations.

We feel that a complete theoretical description of the odd-mass one-hole nuclei with this model would require calculations on the two doubly even neighbors, in order to know more about the nature of their $^12+$ state, the energy of which we are taking as the one-phonon energy. It is probable that this knowledge would allow a better understanding of the levels, particularly those higher than about 2 MeV, which are rather qualitatively accounted for in this and other versions of the SMM. In connection with this, it would be interesting to study if the noted discrepancies are removed by leaving out some approximations, in particular the neglect of anharmonicities.

ACKNOWLEDGMENTS

We are very much indebted to Ing. F. R. Femenia for his important contribution in preparing and performing the computations and for numerous courtesies during the execution of this work.

*Member of the Scientific Career of the Consejo Nacional de Investigaciones Científicas y Técnicas, Argentina.
†On sabbatical leave from Universidad de Oriente, Cumaná, Venezuela.

[1] S. M. Abecasis, O. Civitarese, and F. Krmpotić, in *Proceedings of the International Conference on Nuclear Physics, Munich, 1973,* edited by J. de Boer and H. J. Mang (North-Holland, Amsterdam/American Elsevier, New York, 1973), Vol. 1, p. 86; Phys. Rev. C 9, 2320 (1974).
[2] L. Satpathy and S. C. Gujrathi, Nucl. Phys. A110, 400 (1968).
[3] J. D. McCullen, B. F. Bayman, and L. Zamick, Phys. Rev. 134, B515 (1964).
[4] F. B. Malik and W. Scholz, Phys. Rev. 150, 919 (1966).
[5] J. Vervier, Nucl. Phys. 78, 497 (1966).
[6] J. B. McGrory, Phys. Rev. 160, 915 (1967).
[7] A. Covello and V. R. Manfredi, Phys. Lett. 34B, 584 (1971).
[8] K. W. C. Stewart, B. Castel, and B. P. Singh, Phys. Rev. C 4, 2131 (1971).
[9] J. M. G. Gómez, Phys. Rev. C 6, 149 (1972).
[10] A. Bohr and B. R. Mottelson, *Nuclear Structure* (Benjamin, New York, 1969), Vol. 1.
[11] A. H. Wapstra and N. B. Gove, Nucl. Data A9, 303 (1971).

[12]J. Rapaport, Nucl. Data B3, 103 (1970).
[13]P. H. Stelson and L. Grodzins, Nucl. Data A1, 2 (1965).
[14]A. E. Ball, G. Brown, A. Denning, and R. N. Glover, Nucl. Phys. A183, 472 (1972).
[15]C. M. Lederer, J. M. Hollander, and I. Perlman, *Table of Isotopes* (Wiley, New York, 1967), 6th ed.
[16]V. S. Shirley, in *Tables of Nuclear Moments in Hyperfine Interactions in Excited Nuclei*, edited by G. Goldring and R. Kalish (Gordon and Breach, New York, 1971), p. 1255.
[17]Numerical results will be sent on request to the authors.
[18]G. Alaga, V. Lopac, V. Paar, F. Krmpotić, and L. Sips, Institute Ruder Bosković, Zagreb, Yugoslavia, Report No. IRB-TP-4-73 (unpublished); in *Proceedings of the International Conference on Nuclear Physics, Munich, 1973* (see Ref. 1), Vol. 1, p. 278.
[19]A. E. McGregor and G. Brown, Nucl. Phys. A190, 548 (1972).
[20]The $B(E2)$ and $B(M1)$ values quoted in Z. P. Sawa, J. Blomquist, and W. Gullhomer, Nucl. Phys. A201, 433 (1973), are not too reliable due to the lack of a precise knowledge of mixing and branching ratios.
[21]Z. P. Sawa, J. Blomquist, and W. Gullhomer, Nucl. Phys. A205, 257 (1973).
[22]B. Rosner and C. H. Holbrow, Phys. Rev. 154, 1080 (1967).
[23]A. G. Blair and D. D. Armstrong, Phys. Rev. 151, 930 (1966).
[24]T. R. Fisher, A. R. Poletti, and B. A. Watson, Phys. Rev. C 8, 1837 (1973).
[25]G. Alaga, in *Cargèse Lectures in Physics*, edited by M. Jean (Gordon and Breach, New York, 1969), Vol. 3, p. 575; V. Paar, Nucl. Phys. A185, 544 (1972).